APPROVED FOR PUBLICATION

AUSTRALIAN ATOMIC ENERGY COMMISSION

RESEARCH ESTABLISHMENT
LUCAS HEIGHTS

A PULSED NEUTRON MEASUREMENT IN BeO AND DERIVATION OF THE THERMAL NEUTRON DIFFUSION PARAMETERS FROM THE λ (B^2) CURVE

by

A.I.M. RITCHIE

November 1967

APPROVED FOR PUBLICATION

AUSTRALIAN ATOMIC ENERGY COMMISSION

RESEARCH ESTABLISHMENT

LUCAS HEIGHTS

A PULSED NEUTRON MEASUREMENT IN BeO AND DERIVATION OF THE THERMAL NEUTRON DIFFUSION PARAMETERS FROM THE $\lambda(B^2)$ CURVE

by

A. I. M. RITCHIE

ABSTRACT

The decay constant of the neutron population was measured in BeO assemblies of various sizes. Particular attention was paid to the problem of 'room return', establishment of the asymptotic mode, and the appearance of the continuous mode of decay.

The best fit to the $\lambda(B^2)$ curve gave

$$\lambda_a = (1.954 \pm 0.076) \times 10^2 \text{ sec}^{-1}$$

$$D_o = (1.343 \pm 0.011) \times 10^5 \text{ sec}^{-1} \text{ cm}^2$$

$$C = (4.88 \pm 0.31) \times 10^5 \text{ sec}^{-1} \text{ cm}^4,$$

for BeO density 2.96 g cm^{-3} at a temperature of 22°C. The parameters can be used to derive

Continued...

ABSTRACT (Continued)

$L = 26.22 \pm 0.51$ cm

$\lambda_{tr} = 1.619 \pm 0.013$ cm.

The parameterisation of the $\lambda(B^2)$ curve is discussed in conjunction with the problem of deciding when agreement exists between two separate measurements.

Note:

This work has been submitted to a journal. Further details can be obtained from the author or from the Director of the Research Establishment.

CONTENTS

Continued.....

CONTENTS (Continued)

1. INTRODUCTION

Several measurements on thermal neutron diffusion in BeO have already been made using the pulsed neutron technique (Iyengar et al. 1957, Zhezherun 1964, Cuny et al. 1965, Joshi et al. 1965). The typical error quoted for the diffusion coefficient is better than 2 per cent (see Table 1), but there is up to 20 per cent discrepancy between results.

It was considered worthwhile to carry out a further pulsed neutron measurement paying particular attention to the following considerations:

(1) The decay curve measured must be a property only of the assembly under consideration and not of the assembly coupled to its surroundings. This is normally referred to as the problem of 'room return'.

(2) The asymptotic energy mode must be given sufficient time to become established. The decay will then be exponential, with a decay constant independent of time.

(3) The buckling must not be so large that the continuous spectrum is required to describe the decay of the neutron population (Corngold 1965). If the buckling is too large there is no asymptotic energy mode and the neutron density does not decay exponentially.

The steps taken to ensure that the above conditions were satisfied are described in Sections 4 and 5. Section 6 contains evidence to show that the first condition was almost certainly satisfied.

The validity of parameterising the $\lambda(B^2)$ curve is discussed in Section 7, where it is shown that the parameters derived for the present curve are in good agreement with the two most recent results (Cuny et al. 1965, Joshi et al. 1965), and that the diffusion length derived from the present parameters agrees with that measured by an exponential experiment on the same sample of BeO. However, it is shown that agreement between the sets of parameters can still allow a systematic difference to occur between the $\lambda(B^2)$ curves. Assuming no systematic errors in the time analysers or other equipment, it is pointed out that this systematic difference may be due to differences in the macroscopic scattering properties of the BeO samples.

2. EXPERIMENTAL LAYOUT

2.1 Pulsed Source

The pulsed source was produced by deflecting the beam of a 3 MeV Van de Graaff accelerator. The main deflection was in the top terminal of the accelerator but post-acceleration deflection was used to reduce the background-to-signal level of the pulse from about 5×10^{-4} per cent to less than 10^{-5} per cent (Fraser, Ritchie and Whittlestone 1967).

The B-9(d,n)B-10 reaction used supplies a copious, although not mono-energetic, source of neutrons. The machine was operated throughout the experiment at about 2.5 MV with peak currents in the pulse ranging from 200 to 800 μa. The pulse lengths varied between 350 and 500 μs with repetition times from 4.5 to 12 ms. The high intensity of the initial neutron pulse made it unnecessary to use long pulse lengths for measurements in the larger assemblies.

2.2 Description of Moderator Block and Shielding

The BeO was in the form of a block 60.96 x 60.96 x 60.96 cm made up of tiles 15.24 x 15.24 x 2.54 cm having an average density of 2.877 g cm^{-3}. An aluminium frame (Figure 1) supported sheets of Boral so that they formed a box in which the various assemblies could be built. The assemblies presented a cross section of either 60.96 x 60.96 cm or 30.48 x 30.48 cm to the beam direction and were of a variety of lengths. The sides of the box were designed so that the Boral was always in direct contact with the BeO to avoid the possibility of the lifetime of neutrons in the assembly being increased by any local 'room return' effect. The whole apparatus was set up on an adjustable table so that, by positioning the stack with the neutron source at the centre of one face, asymmetric modes could be suppressed.

The table and apparatus were housed in a double-walled polythene tent about 2.5 x 2.5 x 2.5 m. The temperature of this volume was controlled by a simple air-conditioning unit which held the temperature at 22°C with less than 2°C total variation and variance of about 0.3°C about the mean temperature.

2.3 Shielding of the Block

In order to define the edge of the moderator and produce as closely as possible the ideal of a vacuum boundary condition, the block is usually lined with a strong neutron absorber. As the (γ,n) threshold in BeO is at 1.67 MeV, $\frac{1}{4}$ in. Boral was used as the absorber instead of cadmium. More than 25 per cent

of the γ-rays from neutron capture in cadmium have energies greater than 1.67 MeV and might give rise to a time-dependent background. Boral has the further advantage of being self-supporting.

Room return neutrons could come from the concrete floor under the assembly, any concrete shielding near the assembly, and the air surrounding the assembly. Decay constants in concrete are of the same order as those in BeO and so a thermal absorber will remove the return from concrete, especially at long times after the pulse. However, the mean life in air is about 125 ms, and hence the air may be a significant source of epithermal neutrons during the decay of the thermal pulse in the BeO. It was found experimentally that a layer of about 6 cm of borated paraffin (equal parts of boric acid and paraffin wax), backed up by $\frac{1}{4}$ in. Boral, eliminated a considerable fraction of the 'background' neutrons at long times. Figure 2 shows time distributions measured with and without the borated paraffin shield in position. The background detected appeared to have no time dependence during the times of interest.

3. DETECTION SYSTEM

Enriched BF_3 counters with active lengths of about 12 cm and diameters of 2.54 cm were used as the neutron detectors. The pulses from the counters were fed through AERE Type 1430A preamplifiers and main amplifiers to tunnel diode discriminators. The pulses were differentiated at the input of the preamplifiers to prevent excessive pulse pile-up and d.c. shifts in the main amplifier.

The time analyser was a Laben 512-channel analyser operating in its multi-scale mode. In this mode the 512 channels can be used as 512 sequentially switched scalers, each of which has a 1 μs pulse-pair resolution time. A 4 Mc/s crystal oscillator drove a control unit which provided a suitable wave train to switch the analyser. This unit allowed the use of 32, 64, or 128 channels whose width could be varied from 1 μs to 200 μs by 1 μs steps. As the analyser takes between 16 and 23 μs to transfer information from the scaling unit to its memory the control unit was designed to leave a storage time of 25 μs at the end of each channel. Figure 3 is a block diagram of the pulsed source and the counting equipment.

4. EXPERIMENTAL METHOD

4.1 Decay Constant Measurements

In all the measurements the counter was placed on the top face of the BeO stack. In order to define the spatial region in which the time decay was being

measured, the counter was enclosed in a 0.10 cm cadmium mask fitted with a rectangular slot 10.32 cm long, 2.54 cm wide and about 1.27 cm deep. This meant that the central anode of the counter was some 2.54 cm from the top surface of the BeO. The counter was always placed with its long axis parallel to the beam direction and with the centre of the slot at the centre of the upper face of the stack. This eliminated any asymmetric spatial modes generated in the beam direction.

The top face of the stack was uneven because of slight differences in the dimensions of the individual tiles used to make up the block, the variation in level being a maximum of ± 0.1 cm. The decay constant was measured several times with the counter at varying heights above the surface of the BeO to check for any systematic changes caused by differences in the separation between the BeO surface and the counter. No significant differences could be detected for a height variation of 0.76 cm.

For most measurements 64 time channels were used as this gave good time resolution and yet channels wide enough to obtain reasonable statistics. In all the measurements it was decided to neglect any information obtained in the first 2 ms after the end of the initial neutron pulse. Measurements on graphite (Cuny et al. 1965, Serdula 1963) have indicated that, in systems of large buckling, thermalisation effects are apparent until 2 ms after the end of the pulse, although this waiting time possibly depends on the source energy (Davis et al. 1965). As thermalisation processes should occur more rapidly in BeO, a waiting time of at least 2 ms should be ample for the asymptotic energy distribution to be established. In systems of smaller buckling, however, higher mode contamination defines the waiting time and this was determined for each such system by a rough initial measurement of the decay constant.

When the waiting time for a particular assembly had been established the source intensity was adjusted to give from 1 to 2 per cent dead time corrections in the first few channels of interest, the aim in each individual measurement being to collect some 10^5 total counts in these channels. This aim, together with rate of decay of the system, determined the time over which the decay of the system was measured. The repetition rate and channel widths were then adjusted to cover the whole of the time variation of the neutron population with the last five or six channels measuring mostly background. Thus all the decay constants were measured with similar precision. The only differences between determinations were the number of times each measurement was repeated and the number of time

channels that actually covered the exponentially decaying part of the time distribution.

4.2 Data Analysis

The time distributions were fitted to the expression

$$y_i = A_1 + A_2 \exp(-\lambda t_i),$$

using a suitable computer programme. This used the weighted least squares criterion to determine the best fit, and solved the non-linear Normal Equations by a Taylor Expansion Method. The programme was also designed to fit the data, from progressively later times after the initial pulse, to the end of the measured time distribution. This served mainly to check for possible time dependence in either the decay constant or the background term. It also proved useful in showing at what times after the pulse the higher decay modes become insignificant.

5. RESULTS

As indicated in Section 4.2 above, the decay constant was determined for each assembly as a function of increasing time after the end of the initial pulse. The results can be classified in three ways:

(1) Those in which the value of the decay constant is a constant for a time > 3 mean lives. In these a single exponential is a good description of the decay. A typical example is shown in the bottom curve of Figure 4 (see also Figure 1, Ritchie and Rainbow 1967).

(2) Those in which the value of the decay constant changes rapidly with time and a single exponential is not an adequate description of the decay. The top curve of Figure 4 is an example of this behaviour.

(3) A 'twilight' region, typified by the middle two curves of Figure 4, for which no firm conclusions could be drawn.

These results and their connection with the appearance of a continuous mode, in systems of large buckling, have been discussed by Ritchie and Rainbow (1967). It is sufficient for the present analysis to use them to put an upper bound on the buckling, (about 3.0×10^{-2} cm^{-2} at $\rho = 2.96$ g cm^{-3}) below which one can confidently assign an unambiguous decay constant to a given assembly.

A closer look at the bottom curve of Figure 4 shows that it too can be divided into distinct sections. Initially the value of the decay constant

increases with time, probably owing to the effect of higher modes but possibly because insufficient dead time correction has been made. Thereafter the value is constant within the errors of the determination. The decay constants were determined for thirteen stacks with bucklings from 0.75 x 10^{-2} cm^{-2} to 2.715 x 10^{-2} cm^{-2}. A complete list of the assembly sizes, the associated decay constants and errors is given in Table 2. It can be seen that at higher bucklings the assemblies were chosen so that a cube-like and a slab-like assembly had similar values of buckling, in order to check any possible dependence of the decay constant on shape.

The actual sizes of the assemblies differed by a small amount from their nominal sizes (0.8 mm on length, 0.3 mm on height and width) owing to the small differences in the dimensions of individual tiles. This obviously affects the buckling assigned to each assembly but also effectively changes the density of each assembly under study. The densities calculated for each stack size are given in Table 2, the total variation being about 0.3 per cent. This is significant when compared to the quoted errors on the decay constants of about 0.2 per cent. To overcome this density variation and also to provide results directly comparable with other workers, the decay constants were normalised to unit density and the stack dimensions were measured in units of g cm^{-2} (Table 2).

The normalised decay constants were fitted with a polynomial in the normalised bucklings. The normalised bucklings were obtained using a weighted least squares method, the weight of each point being determined by the error in the decay constant and the error on the buckling. The order of the polynomial fit and the extrapolation length used to calculate the buckling could be varied. The results of various fits using the best value of extrapolation length are given in Table 3.

Also given in Table 3 is the value of the 'Variance of Fit' which can be used as a criterion in deciding the best fit to the data. This parameter is defined as

$$VAR = \sqrt{\sum_i \frac{w_i (y_{ie} - y_{ic})^2}{N-M}} \quad ,$$

where y_{ie} = experimental value at the i^{th} point,
y_{ic} = calculated value at the i^{th} point,
N = number of data points,
M = number of parameters in the fit, and
w_i = weight of the i^{th} point.

If the weights are correct and the fit good, then the parameter VAR should have a value close to unity with the best fit having the least value of VAR.

6. DISCUSSION OF ERRORS

6.1 Error on each Decay Constant Measurement

The following possible sources of error need to be considered in each decay constant measurement:

(1) Random error due to the statistical error in the counts in any time channel.

(2) Random error due to changes in the time analyser channel widths.

(3) Systematic error due to dead-time corrections.

(4) Systematic error due to room return.

The error due to counting statistics at the start of each time distribution was about 0.2 per cent. By comparison the variation in channel width due to the variation in the crystal frequency (0.01 per cent) and variations in the frequency dividing system (estimated to be less than 0.01 per cent) can be neglected.

The dead time of the BF_3 counter and the time analysing system was measured as 1.7 ± 0.8 μs. The decrease in decay constant in changing the dead time from 2 μs or 0 μs was typically 0.05 per cent. Hence it would seem that any systematic error due to incorrect dead-time correction can be neglected.

The effect of room return is much more difficult to assess. Table 4 shows the decay constant of an assembly of relatively large buckling measured at three widely spaced points in time. In the first measurement the main source of reflected neutrons would have been the floor. In the last the reflections from the floor, side walls and roof would have been of the same order. As there does not appear to be any systematic trend within the errors quoted (derived from the statistical counting error only) it can be assumed that there is no systematic error due to room return.

6.2 Errors on Each Point of the $\lambda(B^2)$ Curve

The total error on each point of the $\lambda(B^2)$ curve is compounded from the following:

(1) The error on the decay constant derived from the exponential fitting.

(2) Error on the decay constant due to uncertainty in the channel width.

(3) Variation of the decay constant caused by temperature fluctuations.

(4) Errors on the buckling due to uncertainty in the geometric dimensions.

(5) Variations due to uncertainty in the density of the assembly.

(6) Systematic error due to assuming the wrong density for the assemblies.

The error on the decay constant from the exponential fitting has already been discussed and was typically 0.2 per cent. The channel widths were equal to their nominal channel widths to within 0.02 per cent. The variation of the decay constant caused by temperature drifts during the course of the experiment was estimated to be about 0.05 per cent. The effect of temperature and channel width variation were neglected in assigning an error to the decay constants of the $\lambda(B^2)$ curve.

The error in buckling due to the variation in the dimensions of the stacks was estimated to vary between 0.02 per cent and 0.07 per cent, depending on stack size. Measurement of the densities of individual tiles showed a standard deviation about the mean of about 0.5 per cent. If an assembly is considered to be made up of R tiles chosen at random from N (284 in this case) it can be shown that the root mean square deviation will be $0.5\sqrt{(N-R)/NR}$ per cent. This leads to a value of 0.07 per cent for the smallest assembly and is the same order as the error due to the uncertainty in the dimensions. However, the error decreases rapidly with increasing assembly size, being only 0.04 per cent for the next smallest assembly. In assigning an error to the buckling of a point on the $\lambda(B^2)$ curve the error due to the uncertainty in the density was neglected.

The assumptions about the errors are justified by the value of the Variance of Fit, which indicates that the points on the $\lambda(B^2)$ curve have been weighted correctly (Table 3).

Table 3 also shows the results of fitting polynomials to a curve in which the decay constants and bucklings were normalised to a mean stack density of 2.8665 g cm^{-3} instead of the individual densities given in Table 2. The second order fit was still the best but the value of $\rho\epsilon$ giving the best fit was 3.325 g cm^{-2}, and not the 3.38 g cm^{-2} found when individual stack densities were used. The parameters λ_a, D_o, and C are 2 per cent lower, 0.3 per cent higher and 3.5 per cent higher than the respective values obtained using individual densities. These changes are all significant compared to the quoted errors of 3.8 per cent, 0.8 per cent, and 6.4 per cent. Hence it would seem that it is important to estimate accurately the density of individual stacks and allow for

the voidage that exists when a stack is made up of a number of smaller components.

7. DISCUSSION OF RESULTS

7.1 Parameterisation of the $\lambda(B^2)$ Curve

The results of fitting various order polynomials to the density normalised $\lambda(B^2)$ curve are given in Table 3. Judging by the Variance of Fit a fourth order polynomial is the best fit to the data. However, as the errors on the third and fourth order coefficients are of the same magnitude as the coefficients themselves, the fit is probably an overfit to the data. The best fit is then the second order fit. The rejection of the fourth order fit emphasises one of the major difficulties in the analysis of this type of experiment. Only a portion of the $\lambda(B^2)$ curve can be measured experimentally but the parameterisation of the curve demands that points, in particular the zero buckling intercept, can be determined by extrapolating the polynomial fitted to the curve outside the range of the experimental results. In fact, the fourth order polynomial of Table 3 would be the best fit to use if any interpolation between experimental points was required. Its rejection is due in part to the fact that it does not give the correct zero-buckling behaviour. The experimenter must therefore add rather ill-defined constraints on the curve fitting in addition to the goodness of fit to the experimental points. This introduces a degree of subjectivity which makes difficult the comparison of different experimental results when only the fitted parameters are quoted.

The reasons for fitting the curve to a polynomial appear mostly historical. The early theory (Singwi 1960, Purohit 1961, Nelkin 1960) approached the problem via two-group diffusion theory. It has been pointed out recently (Corngold and Durgun, 1967) that, especially close to the continuum, the curve is unlikely to be a polynomial. For this reason and because of the uncertainty in the physical meaning of the polynomial fit we will emphasise the use of the $\lambda(B^2)$ curve and endeavour to compare our curve with those of other experimenters. The parameters derived from fitting to a polynomial will be discussed only to produce comparisons with work where the $\lambda(B^2)$ curve is not given, and to discuss the effect on the parameters of variations in the extrapolation length.

Table 1 shows the present results, together with previous results, for the diffusion parameters of BeO. All the parameters have been renormalised to a density of 2.96 g cm^{-3} and a temperature of 22°C. The results of Iyengar et al. and Zhezherun were obtained using bucklings much larger than the limiting buckling (B^{*2} about 2.9 x 10^{-2} cm^{-2}) quoted in Section 5, and for this reason will not be

compared in detail with the more recent determinations.

The present value of the diffusion coefficient agrees with the two most recent measurements to within the quoted errors, which are all of about the same order. The agreement between the three values of the diffusion cooling constant is also good although the error in the result of Cuny et al.is very large (about 35 per cent).

The very small absorption cross section (about 10 mb) of BeO makes the value of λ_a very sensitive to impurities. Hence the rather large variation in the parameter indicated by the first column of Table 1 is to be expected. The large value of the present determination is almost certainly caused by surface contamination of the tiles. An early measurement of the diffusion length using a stationary technique (Brittliff et al. 1963) gave a value of 29.9 ± 0.8 cm while a later one (Duerden 1966 - A.A.E.C. unpublished report) carried out immediately after the pulsed measurements gave a value of 26.9 ± 0.7 cm. This latter measurement is in good agreement with the value of 26.2 ± 0.5 cm derived from λ_a and D_o of the present pulsed neutron measurements.

The value of the extrapolation length giving the best fit to a second order polynomial was ϵ = 1.128 cm when normalised to a density of 2.96 g cm^{-3} and allowing an effective thickness of 0.01 cm for the 0.10 cm of aluminium supporting the Boral. This value of the extrapolation length compares well with the value of 1.13 cm found by Joshi and with the value 1.149 ± 0.009 cm derived from the diffusion coefficient and $\epsilon = 0.71\ \Sigma_{tr}$. If the value of the extrapolation length derived from the diffusion coefficient rather than that derived from the best fit to the data is used to calculate the buckling, the magnitudes of the parameters D_o and C are increased by 0.03 per cent and 0.66 per cent respectively. This effect is small compared to the errors in these parameters.

7.2 $\lambda(B^2)$ Curve

Figure 5 shows the present determination of the $\lambda(B^2)$ curve for BeO. The results were normalised to unit density and the absorption term subtracted. The only other set of results available which has been measured over a similar range of buckling and reported in sufficient detail was also normalised to 22°C and unit density and plotted on the same graph. The two curves should therefore be directly comparable.

There appears to be a systematic divergence between the present curve and that of Joshi et al. the difference being about 1.8 per cent at the largest

buckling common to both measurements. In this region the errors on the points are about 0.3 per cent at most, which would indicate that the systematic trend is significant. As the coefficients of the first and second order powers of B^2 agree within their respective errors, there now arises the problem of deciding what constitutes agreement between various experiments. This further emphasises the necessity of comparing $\lambda(B^2)$ curves and not the coefficients derived from these curves.

If we assume that the two curves are different and that the usual sources of systematic error such as density variations of the assemblies and errors in the time analyser widths have been adequately accounted for, then the discrepancy may be due to the different scattering properties of the two BeO samples. This problem has been noted elsewhere (Beckurts 1965, Zhezherun et al. 1964) and can only really be solved by using the same apparatus for measurements on two different samples.

8. CONCLUSIONS

The very accurate timing equipment and the high-intensity low-background pulsed sources now available make it possible to measure decay constants to within 0.1 per cent. However, it now becomes important to define the temperature of the stack to better than 0.5°C and to know the density to much better than 0.1 per cent. This last requirement may be rather stringent as moderators such as BeO, Be and graphite are manufactured by techniques which generally produce samples varying in density by about 0.5 per cent to 1.0 per cent. Hence considerable care would have to be exercised in building a given assembly out of small blocks or measuring the density of one large block. Over and above all this is the problem of possible differences in the macroscopic scattering properties due to variations in methods of manufacture. Hence until this problem is resolved there seems little point in measuring decay constants with better precision that at present, unless one is interested only in a particular batch of moderator.

Unlike the decay constant, or more precisely, the time variation of the neutron density, the buckling is not a real physical property of the system under study, but a mathematical concept introduced to measure the surface leakage of neutrons from the system. Hence there always remains the niggling doubt about the physical significance of a $\lambda(B^2)$ curve. (This problem has been discussed briefly by Wood and Williams 1967). Assuming for the moment the reality of the buckling, and the ability to calculate it for a parallelepiped, its accuracy will also depend on the accuracy with which the density and the dimensions of the system

are known. As the buckling varies inversely as the square of the density in a normalised $\lambda(B^2)$ curve control of the density is even more necessary than for decay constant determinations and would indicate that it is preferable to use single blocks of moderator rather than a stack made up of smaller blocks. The same conclusion holds when considering the dimensions of the system unless the small blocks are tailored to produce a voidless stack with very small surface irregularities. In the present work the errors in the buckling were 0.02 to 0.07 per cent and it would appear that considerable care and forethought would have to be exercised if the buckling was required to a much higher accuracy than this.

9. ACKNOWLEDGEMENTS

We would like to thank the operating team of the Van de Graaff accelerator for their help in running the machine. Thanks are also due to Mr. M. T. Rainbow for considerable help in the experimental work and to Mr. K. J. Maher and Mr. B. McGregor for their help with the various fitting programmes.

10. REFERENCES

Beckurts, K. H. (1965). - I.A.E.A. Conf. on Pulsed Neutron Research, 1 : 3.

Brittliff, E., Duerden, P., and McCulloch, D. B. (1963). - AAEC/TM203.

Corngold, N. (1965). - Nucl. Sci. and Eng. 23 : 403.

Corngold, N., and Durgun, K. (1967). - To be published in Nucl. Sci. and Eng.

Cuny, G., Deniz, V., Lalande, J., LeHo, J. G., and Sagot, M. (1965). - I.A.E.A. Conf. on Pulsed Neutron Research, 1 : 89.

Davis, S. K., De Juren, J. A., and Rier, M. (1965). - Nucl. Sci. and Eng. 23 : 74-81.

Fraser, H. J., Ritchie, A. I. M., and Whittlestone, S. (1967). - AAEC/TM400.

Iyengar, S. B. D., Mani, G. S., Ramanna, R., and Umakanth, N. (1957). - Ind. Acad. of Sci. Proc. (A) 45 : 215-223.

Joshi, B. V., Nargundkar, V. R., and Subbarao, K. (1965). - I.A.E.A. Conf. on Pulsed Neutron Research, 1 : 105.

Nelkin, M. (1960). - Nucl. Sci. and Eng. 7 : 210.

Purohit, S. N. (1961). - Nucl. Sci. and Eng. 9 : 305.

Ritchie, A. I. M., Rainbow, M. T. (1967). - Nucl. Sci. and Eng. 28 : 301.

Serdula, K. J. (1963). - Ph.D. Thesis (Birmingham University).

Singwi, K. S. (1960). - Archiv for Fysik 16 : 385-411.

Wood, J., and Williams, M. M. R. (1967). - J. of Nucl. Energy 21 : 113-130.

Zhezherun, I. F., Krasin, A. K., Plindov, G. I., Sadikov, I. P., Tarabonko, V. A., and Chernyshev, A. A. (1964). - Proc. 3rd U.N. Int. Conf. P.U.A.E., P/362a.

Zhezherun, I. F. (1964). - J. Nucl. Energy 18 : 279.

TABLE 1

COMPARISON OF THE MEASURED DIFFUSION PARAMETERS OF

BeO NORMALISED TO A DENSITY OF 2.96 g cm^{-3} AND A TEMPERATURE OF 22°C

Reference	λ_a (sec^{-1})	D_o (sec^{-1} cm^2)	C (sec^{-1} cm^4)	L (cm)	λ_{tr} (cm)	Experimental Conditions
Zhezherun 1964	1.856 ± 0.060 x 10^2	1.473 ± 0.015 x 10^5	3.46 ± 0.23 x 10^5	28.17 ± 1.0	1.77 ± 0.02	ρ = 2.79 g cm^{-3}, Temp. 20°C, 0.5 x 10^{-2} cm^{-2} ≤ B^2 ≤ 9.5 x 10^{-2} cm^{-2}
Cuny et al. 1965	1.450 ± 0.030 x 10^2	1.328 ± 0.02 x 10^5	4.20 ± 1.5 x 10^5		1.59 ± 0.03	ρ = 2.96 g cm^{-3}, Temp. 21.5°C, 0.15 x 10^{-2} cm^{-2} ≤ B^2 ≤ 0.65 x 10^{-2} cm^{-2}
Joshi et al. 1965	1.56 ± 0.043 x 10^2	1.324 ± 0.013 x 10^5	4.81 ± 0.58 x 10^5	29.13 ± 0.44	1.595 ± 0.016	ρ = 2.95 g cm^{-3}, Temp. 24.15°C, 0.28 x 10^{-2} cm^{-2} ≤ B^2 ≤ 2.44 x 10^{-2} cm^{-2}
Present Results	1.954 ± 0.076 x 10^2	1.343 ± 0.011 x 10^5	4.88 ± 0.31 x 10^5	26.22 ± 0.51	1.619 ± 0.013	Mean ρ = 2.867 g cm^{-3} but see text, Temp. 22°C, 0.75 x 10^{-2} cm^{-2} ≤ B^2 ≤ 2.8 x 10^{-2} cm^{-2}
Iyengar et al. 1957	1.314 ± 0.026 x 10^2	1.17 ± 0.02 x 10^5	3.84 ± 0.08 x 10^5			ρ = 2.96 g cm^{-3}, Temp. 24°C, 1.99 x 10^{-2} cm^{-2} ≤ B^2 ≤ 6.1 x 10^{-2} cm^{-2}

TABLE 2

LIST OF ASSEMBLY SIZES,

WITH ASSOCIATED BUCKLINGS, DECAY CONSTANTS AND DENSITIES

Nominal Length (cm)	B^2 (cm^{-2} x 10^2)	λ (sec^{-1} x 10^{-3})	$\delta\lambda$ (sec^{-1})	B^2/ρ^2 (cm^4 g^{-2} x 10^3)	λ/ρ (sec^{-1} g^{-1} cm^3 x 10^{-2})	$\delta\lambda/\rho$ (sec^{-1} g^{-1} cm^3)	Density ρ (g cm^{-3})
Assemblies with a nominal cross section 60.96 x 60.96 cm							
60.96	0.7375	1.1857	2.8	0.8951	4.1306	0.98	2.8705
55.88	0.7821	1.2393	2.0	0.9494	4.3178	0.70	2.8702
45.72	0.9175	1.4146	2.8	1.114	4.9303	0.98	2.8692
35.56	1.1754	1.7423	2.6	1.429	6.0756	0.91	2.8677
33.02	1.2768	1.8764	3.6	1.553	6.5241	1.26	2.8671
30.48	1.4025	2.0290	7.6	1.707	7.0783	2.65	2.8665
27.94	1.5611	2.2342	4.6	1.901	7.7961	1.60	2.8658
25.40	1.7650	2.4718	10.8	2.150	8.6276	3.73	2.8650
22.86	2.0333	2.7973	7.4	2.479	9.7674	2.58	2.8639
20.32	2.3963	3.2028	4.7	2.924	11.188	1.64	2.8626
Assemblies with a nominal cross section 30.48 x 30.48 cm							
55.88	2.1187	2.8869	5.3	2.574	10.062	1.85	2.8692
40.64	2.3602	3.1547	6.8	2.870	11.002	2.37	2.8675
30.48	2.7387	3.5885	4.7	3.335.	12.523	1.64	2.8655

NOTE: (1) The measured lengths were 0.083 cm greater than nominal

(2) The measured height and widths were 0.03 cm and 0.02 cm greater than nominal for the 60.96 x 60.96 cm and 30.48 x 30.48 cm assemblies respectively.

TABLE 3

COEFFICIENTS DERIVED FROM VARIOUS POLYNOMIAL FITS

TO THE NORMALISED $\lambda(B^2)$ CURVE

POINTS OF CURVE NORMALISED TO BOTH INDIVIDUAL AND AVERAGE DENSITIES

Order of Polynomial Fit	λ_a/ρ ($sec^{-1}\ g^{-1}\ cm^3$) $\times 10^{-1}$	$D_c\rho$ ($sec^{-1}\ g\ cm^{-1}$) $\times 10^{-3}$	$C\rho^3$ ($sec^{-1}\ g^3\ cm^{-5}$) $\times 10^{-7}$	$F\rho^5$ ($sec^{-1}\ g^5\ cm^{-9}$) $\times 10^{-8}$	$G\rho^7$ ($sec^{-1}\ g^7\ cm^{-13}$) $\times 10^{-12}$	VAR	Comments
1	10.482 ± 0.085	3.484 ± 0.005				4.824	Individual densities used to normalise points of $\lambda(B^2)$ curve. $\rho\epsilon$ = 3.38 gives best fit.
2	6.60 ± 0.26	3.976 ± 0.032	- 1.266 ± 0.080			1.080	
3	7.03 ± 0.74	3.897 ± 0.133	- 0.822 ± 0.728	- 7.5 ± 13.2		1.120	
4	14.58 ± 2.84	2.080 ± 0.67	14.3 ± 5.5	525.0 ± 188.0	6.2 ± 2.3	0.682	
1	10.505 ± 0.085	3.477 ± 0.005				5.001	Average density of ρ = 2.8665 g cm^{-3} used to normalise $\lambda(B^2)$ curve. $\rho\epsilon$ = 3.33 gives best fit.
2	6.47 ± 0.26	3.987 ± 0.032	- 1.310 ± 0.080			1.120	
3	6.50 ± 0.74	3.982 ± 0.133	- 1.28 ± 0.73	- 0.49 ± 12.2		1.180	
4	14.63 ± 2.86	2.030 ± 0.68	14.91 ± 5.6	-553.0 ± 188.0	6.6 ± 2.3	0.697	

TABLE 4

COMPARISON OF DECAY CONSTANTS

FOR A 60.96 x 60.96 x 22.86 cm ASSEMBLY ($B^2 = 2.033 \times 10^{-2}$ cm^{-2})

WITH VARIOUS CONFIGURATIONS OF CONCRETE SHIELDING

Date	$\lambda(sec^{-1}) \times 10^{-3}$	$\delta\lambda(sec^{-1}) \times 10^{-3}$	Concrete Configuration
16/10/65	2.8008	0.0027	Floor 2 feet below stack. 
12/12/65	2.7973	0.0076	Floor + 2 feet of concrete 2 feet from stack near target. 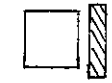
14/ 4/67	2.8046	0.0030	Floor + concrete at target + 2 feet of concrete 3 feet from roof of assembly and 2 feet of concrete 3 feet from the sides nearest the target. 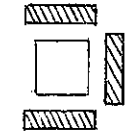

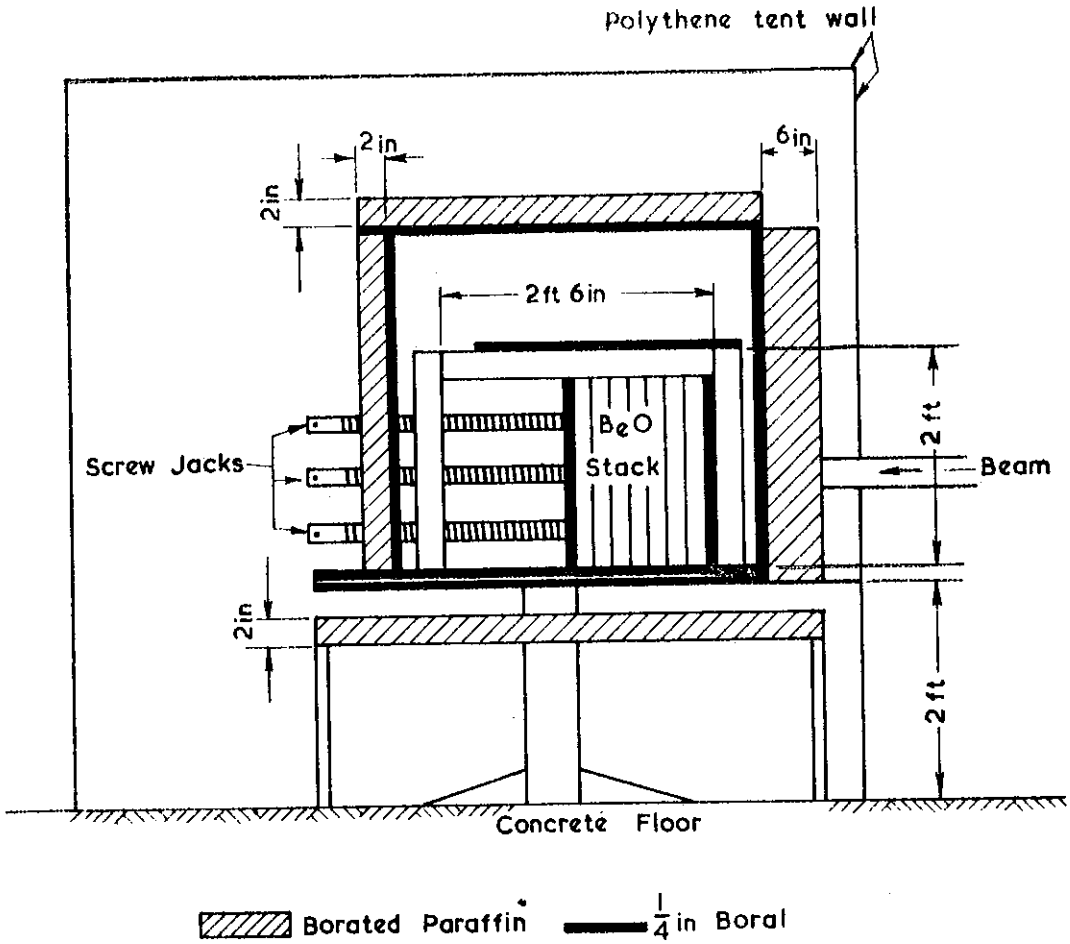

FIGURE 1. SCHEMATIC DIAGRAM OF BERYLLIUM STACK AND ASSOCIATED SHIELDING

P1224

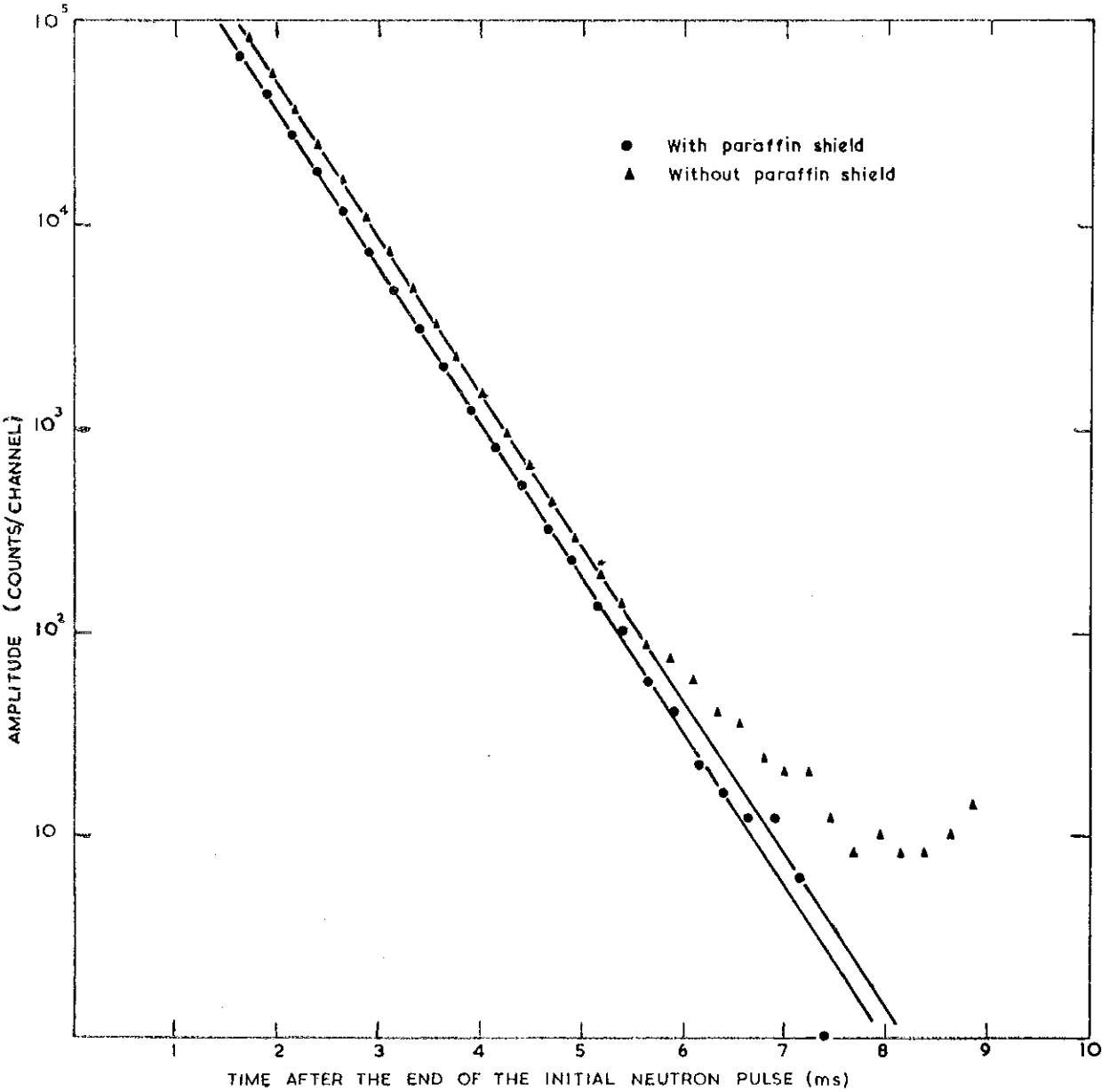

FIGURE 2. COMPARISON OF THE TIME BEHAVIOUR OF THE NEUTRON POPULATION IN A STACK HAVING A BUCKLING OF 1.175×10^{-2} cm^{-2} WITH AND WITHOUT A BORATED PARAFFIN SHIELD

P1224

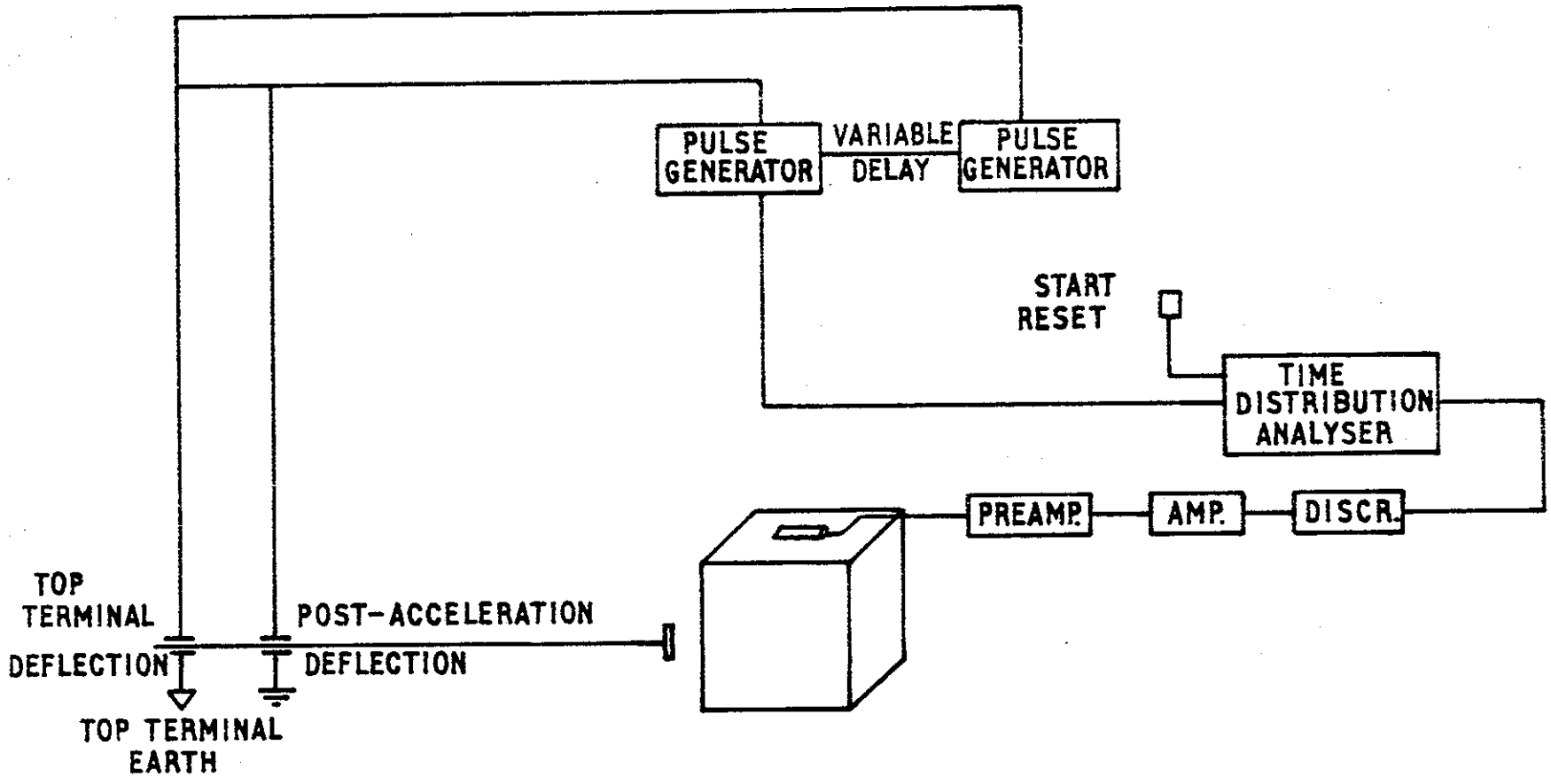

FIGURE 3. ELECTRONICS AND TIMING SYSTEM FOR MEASURING TIME DISTRIBUTION IN BERYLLIUM OXIDE

P1224

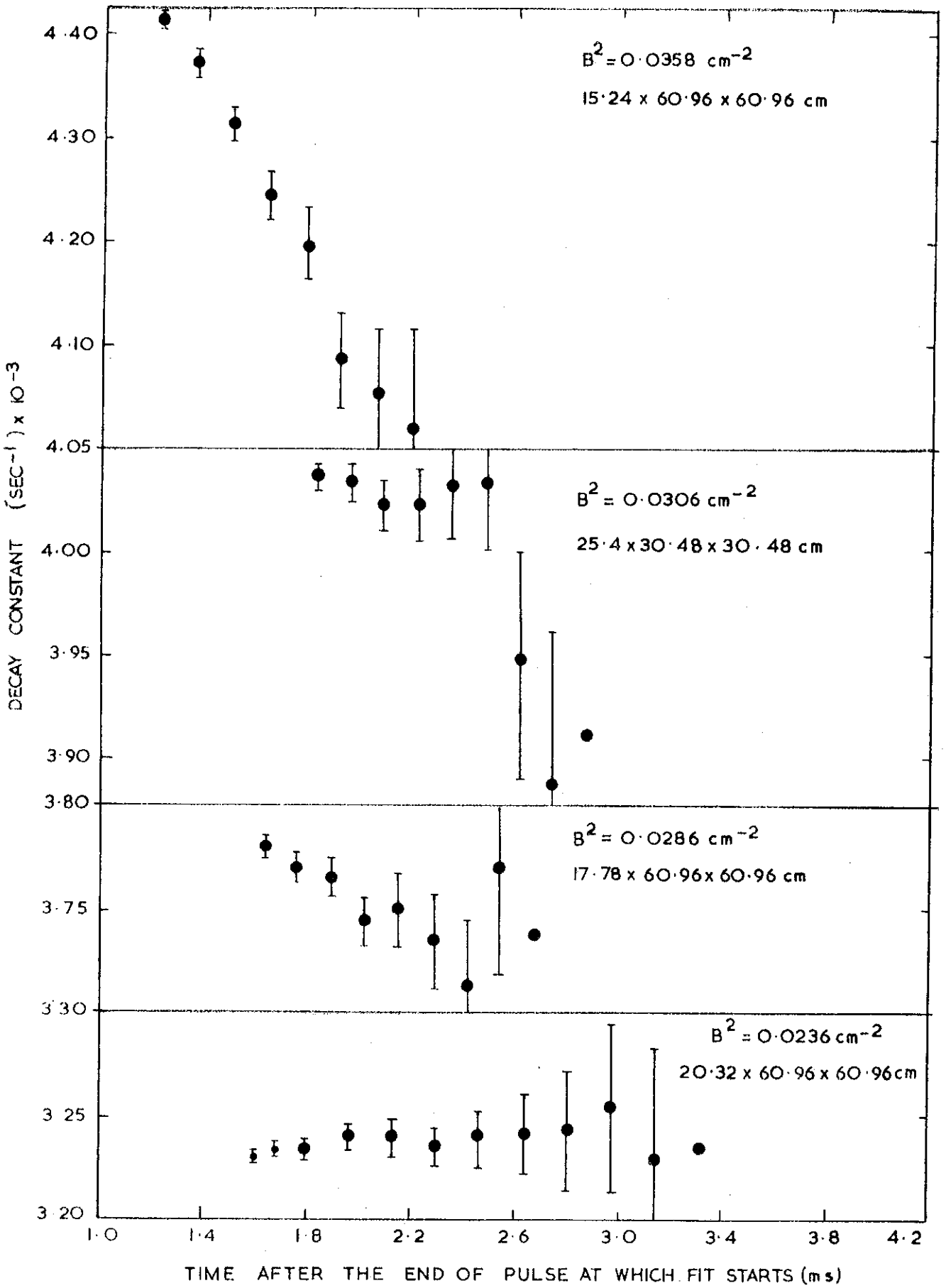

FIGURE 4. VARIATION OF FITTED DECAY CONSTANT WITH TIME FOR VARIOUS SIZES OF ASSEMBLY

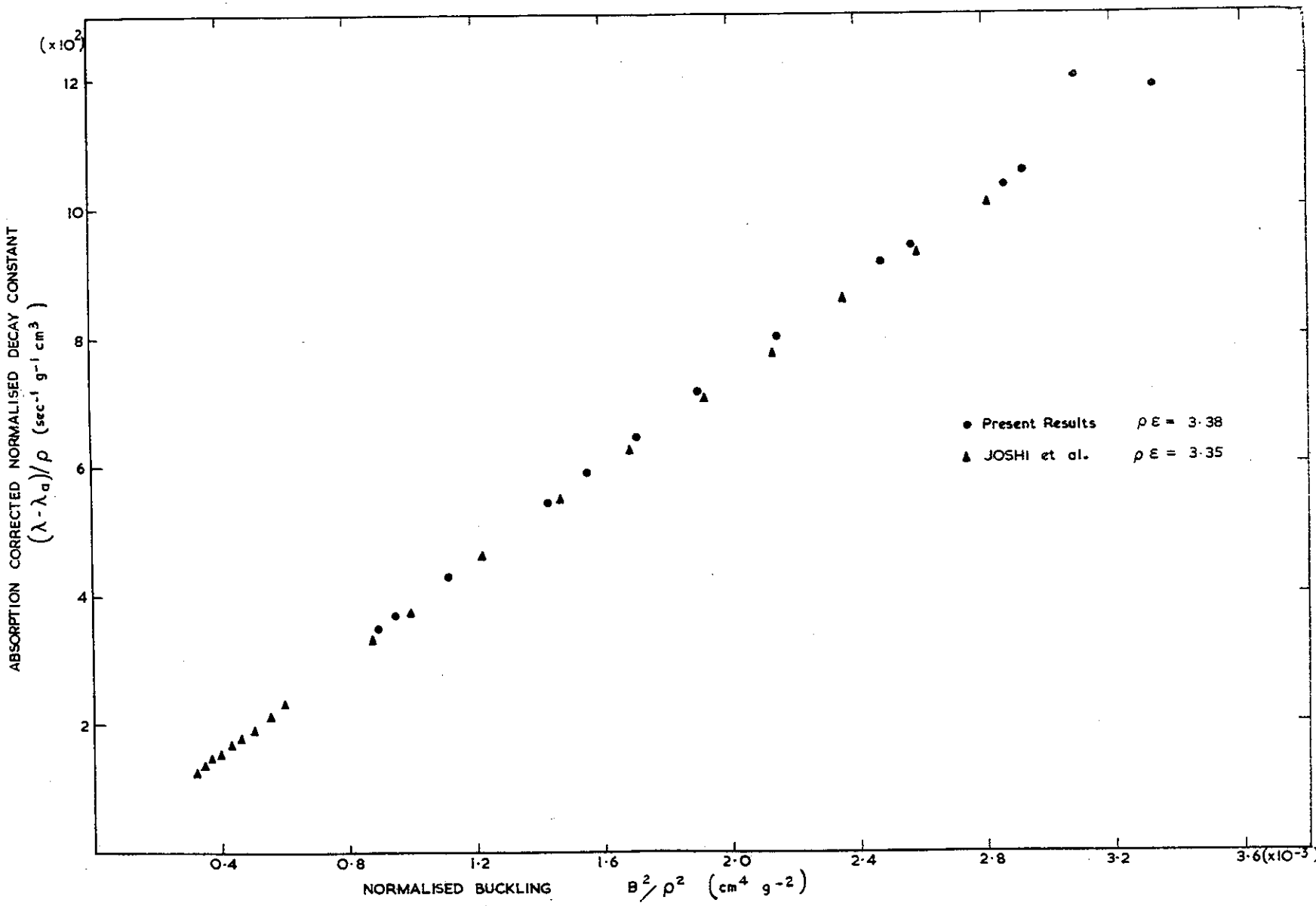

FIGURE 5. COMPARISON OF DENSITY AND TEMPERATURE NORMALISED λ (B^2) CURVES

P1224